Research Article

Comparative Study between Multiwall Carbon Nano Tube and Carbon Waste from Aluminium Production in the Preparation of Thermally Stable Cementitious Mortar

Hisham M. Khater[1]*, Mahmoud Gharieb[1]

[1]Instuite of Raw Building Materials and Processing Technology, Housing and Building National Research Centre (HBRC), Cairo, Egypt

*Correspondence to: Hisham M. Khater, PhD, Professor, Instuite of Raw Building Materials and Processing Technology, Housing and Building National Research Centre (HBRC), 87 El-Tahreer St., Dokki, Giza, P.O., 11511, Egypt; Email: Hkhater4@yahoo.com

Abstract

Objective: The objective of this study is to conduct a comparative investigation into the performance of multiwall carbon nanotube (MWCNT) and carbon wastes (C-waste) derived from the aluminum industry in the creation of thermally stable cementitious mortar. Specifically, the research aims to assess their impact on compressive strength and thermal stability, with a focus on identifying the superior additive for enhancing the properties of cement mortar.

Methods: Cement mortar is produced using a blend of CEMIII cement and sand passing through a 1 mm sieve. Various ratios of MWCNT and C-waste, ranging from 0.1% to 0.7%, are incorporated into the mixture. Compressive strength tests are conducted at different intervals, up to 90 days, to evaluate the effects of additives on strength enhancement. Additionally, the resistance to high temperatures is examined by subjecting the mortar samples to firing temperatures up to 700 degrees Celsius.

Results: The inclusion of both MWCNT and C-waste leads to improvements in compressive strength values, with the most significant enhancement observed at 0.1% concentration, resulting in approximately 70MPa and 75MPa at 90 days, respectively. Notably, C-waste demonstrates superior physical and mechanical properties compared to MWCNT, along with a lower production cost. Moreover, both additives exceed the specified limits for thermal resistance in mortar, achieving measurements of about 60MPa for MWCNT and 63MPa for C-waste when exposed to firing temperatures of 700 degrees Celsius. These results highlight the higher thermal stability of C-waste relative to MWCNT.

Conclusion: In conclusion, this study confirms the efficacy of utilizing C-waste as an additive in cementitious mortar production, showcasing its superior performance over MWCNT in terms of compressive strength enhancement and thermal stability. The findings underscore the potential of repurposing industrial by-products such as C-waste to improve material properties while also addressing environmental concerns and reducing production costs in construction applications.

Keywords: sustainable, activation, composites, eco-friendly, nano, C-waste

1 INTRODUCTION

Nano-engineering of cement involves the inclusion of nano-sized building blocks, which can serve as nucleation sites and fillers within the concrete, thereby enhancing the internal porosity and promoting a more uniform distribution of the material. Previous studies have primarily focused on the utilization of nanoparticles such as nano-SiO_2, nano-$CaCO_3$, and nano-TiO_2[1].

Carbon nanotubes (CNTs), can be either single-walled or multi-walled in structure. A single-walled nanotube consists of a single graphene sheet rolled into a cylinder, while a multi-walled nanotube (MWNT) comprises multiple layers of graphene sheets rolled coaxially around a hollow core[2-4].

Chaipanich et al.[5] conducted a study to examine the impact of incorporating CNTs at 0.5% and 1% by weight in a fly ash cement matrix on the mechanical properties of CNT-fly ash cement composite. The results indicated that the addition of CNTs aided in further filling the gaps between the hydration products, such as calcium silicate hydrates (CSH) and ettringite.

Nochaiya and Chaipanich[6] examined the microstructure properties of a composite material consisting of Portland cement and multi-walled carbon nanotubes. Multi-walled CNTs were used as an additive material, at a weight percentage of up to 1% of cement. The findings demonstrated a favorable interaction between the multi-walled carbon nanotubes and the hydration products of Portland cement pastes, with the multi-walled carbon nanotubes serving as fillers.

Morsy et al.[7] conducted an investigation into the behavior of the cementitious matrix, which was composed of multi-walled carbon nanotubes and nano-clay materials. In this study, a substitution of 6% of nano metakaolin (NMK) by weight was made for the ordinary portland cement (OPC), and mortar samples were subsequently prepared. Analysis of the scanning electron micrographs revealed a densely packed structure in the NMK cement mortar, with the presence of calcium hydroxide in the form of ill-crystals.

Li et al.[8] carried out a study to investigate the impact of incorporating multiwall carbon nanotube (MWCNT) on the properties of cement mixtures. The results indicated that the use of carbon nanotubes can enhance the compressive strength of cement. Specifically, the compressive strength was found to increase by up to 19% when carbon nanotubes were added.

Mudasir and Naqas[9] examined the physical and mechanical properties of concrete that contained 0.5% CNTs by weight of cement. These CNTs were incorporated into concrete mixes with different water cement ratios, namely 0.40, 0.45, 0.48, and 0.50. The findings of this study revealed that at a water cement ratio of 0.45, the compressive strength, split tensile strength, and moment of resistance were greater by 8.89%, 28.9%, and 5.33% respectively, when compared to the reference mixes. However, it should be noted that the workability of the concrete was diminished by 38.40%, and the water absorption decreased by 0.03%.

There is a positive interaction between carbon nanotubes and the fly ash cement matrix, resulting in a denser microstructure and increased strength compared to fly ash mix without CNTs. The compressive strength of fly ash mixes increases with the content of carbon nanotubes, with the highest strength achieved at 1% by weight of CNTs. Furthermore, the inclusion of CNTs leads to an increase in compressive strength under high strain loading rate[10,11].

In a study by Chen et al.[12], a comprehensive review on CNT-cement composites was presented, along with an analysis of the impact of concentrated CNTs on properties of Portland cement, including fabrication, hydration, mechanical properties, porosity and transport, conductivity, and piezo-resistivity. The authors also discussed different methods of CNT dispersion in cement and their influence on mechanical and electrical charge properties.

Carbon nanotubes have the potential to significantly enhance the performance of concrete at elevated temperatures by improving the fracture performance and early strain capacity of cement paste and mortar, as well as reducing crack propagation at high temperatures[13]. The mechanical properties of concrete with varying carbon nanotube contents were investigated by Yao and Lu[14] at room temperature, 300°C, 600°C, and 900°C. It was observed that the compressive strength of carbon nanotube concrete initially increased and then decreased at different temperatures.

Khater and Naggar[15] conducted a study on the effect of multi-walled carbon nanotubes (MWCNT) on the resistance of alkali-activated composites to chloride attack. The results demonstrated that the composites with MWCNTs exhibited high resistance and stability against magnesium chloride solution. Furthermore, the mixes with glass waste had higher mechanical strength compared to those with silica fume.

Khater and Naggar[16] also conducted a study where they produced and characterized sustainable geopolymer

Figure 1. Mineralogical composition of starting raw materials. [Q: Quartz (SiO_2), O: Orthoclase[KAl_3O_8]; C_2: Larnite, C_3: C3S].

composites that have a high potential to resist sulfate attack. These eco-friendly composites were made from metakaolin and blast furnace slag, with the addition of 10% silica fumes or glass waste powder as control mixes. Additionally, they incorporated Multiwall carbon nanotube (MWCNT) in varying percentages (0.01% to 0.09% by weight). The inclusion of MWCNT resulted in an increased sulfate resistance of up to 0.07% for both matrices incorporating glass waste or silica fume. This finding highlights the sustainability of these composites in marine environments.

Saafi et al.[17] investigated the impact of different ratios of MWCNTs on the electrical and mechanical properties of fly ash-geopolymeric composites. The results showed a significant improvement in flexural strength, flexural toughness, and young's modulus, with an increase of up to 160%, 275%, and 109% respectively, when MWCNT was added. Additionally, the electrical conductivity was enhanced by approximately 200%. Similarly, Khater and Gawwad[18] studied the effect of different MWCNT ratios on the characteristics of geopolymeric mortar.

In the present study, we examine the enhancement effects of carbon wastes (C-waste) in comparison to multiwall carbon nanotubes, at different ratios, on the mechanical properties of cement pastes cured in tap water. Additionally, we investigate the impact of these materials on the compressive strength and microstructure of cement pastes at high temperatures using XRD and differential thermal gravimetric (DTG) analysis.

2 MATERIALS AND METHODS
2.1 Materials
The binder utilized in this research consist of blended cement (CEMIII) 42.5 N, which adheres to ASTM C-150[19]; [Suez cement co. Egypt], as well as fine sand dunes. The mineralogical compositions of the initial raw materials are indicated in Figure 1, whereas the chemical composition assigned in Table 1. It can be observed that CEMIII primarily consists of tricalcium silicate (C3S) and dilcalcium silicate,

whereas the sand dunes are primarily composed of quartz sand. MWCNT employed in this study were prepared through the use of a CVD instrument at nano-technology lab -HBRC center in Egypt. The main physical properties for MWCNTs are assigned in Table 2.

The physico-chemical properties of the C-waste materials are outlined in Table 3. These materials primarily consist of iron, calcium, sodium, silica, and titanium, with decreasing order of abundance. The C-waste possesses an ash content of up to 4% and a fixed carbon content of 98%. Figure 2 provides a comprehensive comparison of the microstructures of MWCNT and C-waste using transmission electron microscopy (TEM) instrument. It is evident that both materials exhibit nano-sized structures. While MWCNT displays a distinct tubic structure with a particle size ranging from 20 to 24nm, the C-waste features fumed carbon particles with sizes ranging from 25 to 47nm, with only slight indications of tubic structures similar to MWCNT.

2.2 Dispersion of MWCNTs
MWCNTs, along with C-waste materials, were initially combined with Gelnium Ace 30-polycarboxylate-based superplasticizer and 50% of the added water. This particular superplasticizer has been scientifically demonstrated to effectively disperse CNTs[20,21]. The ensuing solution underwent sonication for a duration of 15min utilizing a Fritish 450 Sonifier Analog Cell Distributor[22]. Solutions with concentrations of 0.1, 0.3, 0.5, 0.7, and 0.9wt. %, relative to the total weight of the matrix, were employed to ascertain the optimal concentrations of MWCNTs and their resistance to a corrosive environment.

2.3 Samples Preparation and Curing Regime
The molding and curing procedures are executed in accordance with the subsequent steps:

The binding mortar was enhanced by MWCNT in the amount of 0.7wt. % of the binder weight, as opposed to having no MWCNT.

(2) In order to enhance the dispersion, the MWCNT particles underwent a 15-min sonication process, employing a reduced quantity of water and the employed superplasticizer, while simultaneously upholding a temperature of 40°C.

(3) All raw materials, also known as precursors, were passed through a 90μm sieve, as indicated in Table 4, followed by 10min manual mixing. Subsequently, a rotary mixer was employed for an additional 5min.

(4) The combination of carbon nanotube and superplasticizer was introduced and thoroughly blended with the mixture.

(5) The resultant paste mixtures were cast into cubic-shaped molds with a length of 2.5cm. These molds were then subjected to compaction by shaking, sealed with a lid, and left at room temperature for a duration of 24h.

Table 1. Chemical Composition of Starting Materials (Mass, %)

Oxide Content (%)	SiO$_2$	Al$_2$O$_3$	Fe$_2$O$_3$	CaO	MgO	SO$_3$	K$_2$O	Na$_2$O	TiO$_2$	MnO	P$_2$O$_5$	Cl-	SrO	BaO	L.O.I.	Total	Cl-
CEMIII (42.5N SUEZ CO.)	24.16	8.17	3.04	54.78	4.14	2.33	0.44	00.29	00.85	00.56	00.07	--	--	--	1.100	99.92	0.06
Fine Sand (Sand dunes)	89.91	2.00	1.45	1.56	1.91	0.87	0.37	0.06	0.03	0.04	0.03	0.12	--	--	1.65	99.98	--

Table 2. Properties of CNTs Synthesized by Using CVD Apparatus

Amorphous Carbon / %	Surface Area / m^2.g^{-1}	Purity / %	Ash / %	Length / μm	Inner Diameter / nm	Aspect Ratio / %
0	>300	97	3	1-5	20-30	120

Table 3. Physico-chemical Properties of Carbon Waste Materials Produced from Aluminum Production Industry

Atom	S	Si	Ca	Fe	Ni	V	Na	Ti
Atomic composition in PPM	1.5-2.0	400-500	800-1000	1000-1300	250-350	350-400	600-800	100-200

Physical properties		
Ash content, %	Volatile matter, %	Fixed carbon, %
3.20- 4.0	0.60	96-98
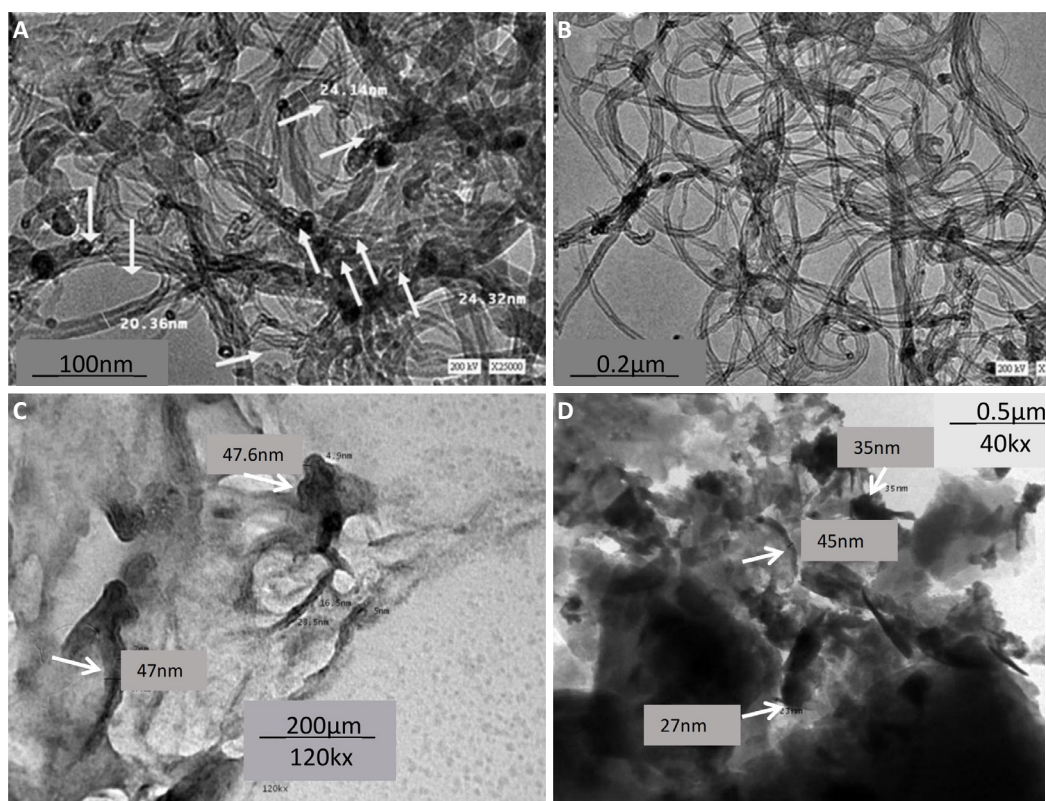
Figure 2. TEM of MWCNT (A, B), and C-waste (C, D).

Following this, the molds were demolded and subjected to a curing process at 40°C with a relative humidity (R.H.) of 100% for a period of 28 days[23].

(6) At the predetermined date, the strength was measured. Meanwhile, the crushed cubes were halted in order to prevent further hydration using the acetone/methyl alcohol method (1:1)[24,25].

(7) The determination of firing resistance was conducted

Table 4. Composition of the Geoplymer Mixes (Mass, %)

Mix No.	CEMIII, %	Sand Dunes, %	C-Waste, %	MWCNT Addition from the Added Binder, %	W/B Ratio, %	Super-plasticizer of the Total Wt., %
R	50	50	--	0.0	0.121	1.2
1	50	50	--	0.1	0.132	1.2
2	50	50	--	0.3	0.139	1.4
3	50	50	--	0.5	0.139	1.6
4	50	50	--	0.7	0.150	1.8
5	50	50	0.1	--	0.126	1.2
6	50	50	0.3	--	0.126	1.4
7	50	50	0.5	--	0.129	1.6
8	50	50	0.7	--	0.129	1.8

through subjecting the specimens to a curing procedure at a temperature of 40°C and a relative humidity of 100% for a period of 28 days. Following this, the specimens were extracted from the curing regime, subjected to drying at a temperature of 80°C for a duration of 24h, and subsequently subjected to calcination at various temperatures ranging from 300 to 700°C for a period of 2h, with a heating rate of 5°C per minute (Guo et al.[26]).

2.4 Exploration Techniques

The utilized raw materials were examined in terms of their chemical composition utilizing the Axios (PW4400) WD-XRF Sequential Spectrometer, a device manufactured by Panalytical in the Netherlands. To determine the mechanical compressive strength of the solidified samples, a 5 t pressing machine (German Brüf) was used, with a rate of 100 kg/min as indicated in Ref[19]. An investigation was undertaken to analyze the diffraction of X-rays (XRD) employing a Philips PW 1050/70 Diffractometer equipped with a Cu-Kα radiation source, spanning an angular range from 0 to 50 degrees 2Θ.

Bulk density was evaluated in accordance with the Equation (1)[27-30]:

$$Bulk\ Density = D/(W\_S)\ (g/cm^3)\ (1)$$

With:

D: The weight of the specimen

S: The weight of the suspended specimen in water

W: the weight of the soaked specimen suspended in air

Strength change factor (SCF) of the solidified samples was calculated utilizing the Equation (2)[31-33]:

$$SCF = 100*(Fi\_Ff)/Fi\ (2)$$

With:

Fi: The 28-day compressive strength of the unfired specimen

Ff: compressive strength of the fired specimen at the designated temperature

The process of thermogravimetry was conducted utilizing the DT-50 Thermal Analyzer, which is a device manufactured by Schimadzu Co-Kyoto, Japan. The specimens were crushed and promptly transferred to an alumina crucible within a nitrogen environment, where N_2 was flowing at a rate of 200mL/min. Subsequently, the specimens were subjected to heating at a rate of 10°C/min in the same gaseous environment, reaching a temperature of 1000°C.

3 RESULTS AND DISCUSSION
3.1 X-ray Diffraction (XRD)

XRD patterns of cement mortar mixes blended for 28 days, containing different ratios of multi-walled carbon nanotubes (MWCNT) and C-waste materials (0, 0.1, 0.3wt. %), and immersed in a solution of magnesium sulfate, are presented in Figures 3A and 3B. The patterns illustrate the continuous formation and growth of CSH with both additives up to a concentration of 0.1%, accompanied by a growth in the amorphous content. However, a further increase in concentration leads to a decrease in CSH formation and growth in crystallinity. This can be linked to the agglomeration caused by higher levels of C-waste and MWCNT, resulting in reduced interaction between the reacting binder and a limited amount of CSH formation, as well as a lower consumption of liberated portlandite, indicating the progress of the hydration reaction. Additionally, MWCNTs and C-waste materials provide different sites for nucleation of crystal growth, as reported in previous literature[34,35], where the hydration products grow on the surface of carbon nanotubes. The binding of CSH phases to MWCNTs occurs at the carboxyl sites through interaction with Ca^{2+} ions in the pore solution. Consequently, the density of carboxyl groups on the surface of MWCNTs can influence the chain lengths of the formed CSH phases.

Upon firing the hardened mortar pastes incorporating 0.1% of both additives, dehydration of CSH and portlandite phases occurs at temperatures exceeding 500 degrees Celsius. Notably, a small peak corresponding to dicalcium silicate, which possesses latent hydraulic properties, is observed, suggesting potential firing resistance for the
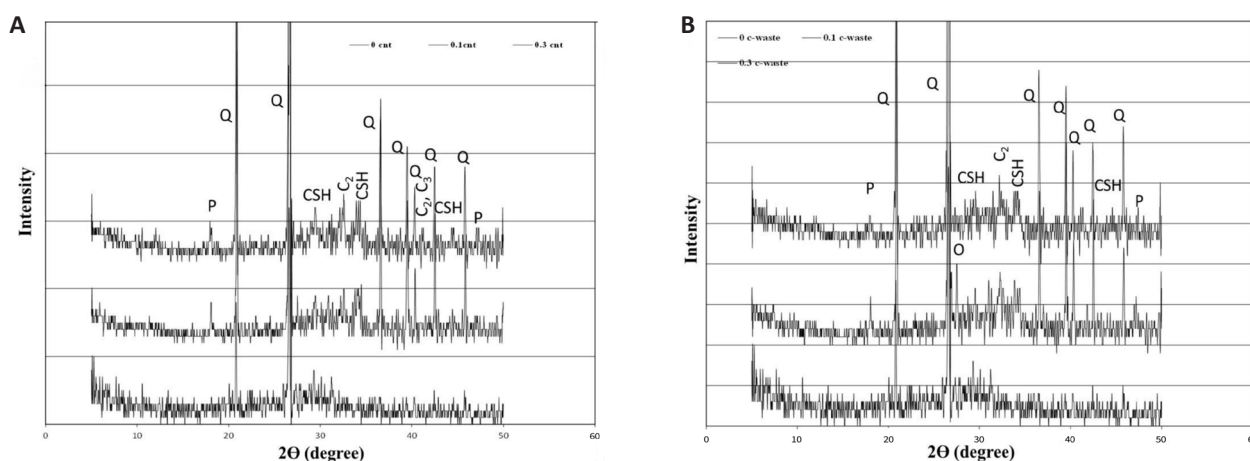
Figure 3. XRD pattern of 28 days CEMIII mortar mixes having. A: Various MWCNT doses. B: Various Nano-carbon wastes. [Q:Quartz, P:Portlandite, C2:dicalcium silicate, CSH: Calcium silicate hydrate, C3: tri calcium silicate, O: Orthoclase]

formed phases at temperatures up to 700 degrees Celsius, as depicted in Figure 4[26,33,36].

3.2 DTG Analysis

Figure 5 illustrates the TGA/DTG thermograms of MWCNT enhanced pastes with various MWCNT and nano C-waste, tap water cured for a duration of 28 days. The thermograms of the CEMIII pastes, with varying amounts of 0, 0.1, and 0.3% MWCNT and nano C-waste (Figures 5A and 5B), exhibit four distinct endothermic peaks in the DTG analysis. These peaks are observed within temperature ranges of 70, 90-180, 450-500, and 680-750°C. The endothermic peaks below 70°C are attributed to the loss of evaporable water. The endothermic peaks observed at approximately 90-180°C are associated with the decomposition of CSH overlapped with calcium sulphoaluminate hydrates (ettringite), as well as calcium alumino-silicate hydrates. The endothermic peak at about 450-500°C is characteristic of the decomposition of portlandite. Finally, the endotherms located at 680-750°C are related to the calcination of calcite ($CaCO_3$).

Figures 5A and 5C depict the increase in intensity of the endothermic peak at around 90-170°C with an increase in MWCNT and nano C-waste up to a concentration of 0.1%. This is accompanied by a sharp rise in the endothermic peak for CSH overlapped with ettringite. Additionally, the endothermic peak at approximately 450-500°C is indicative of the calcium hydroxide decomposition. The intensity of this endothermic peak diminishes as the concentration of MWCNT and nano C-waste increases, indicating the enhanced activation efficiency of MWCNT and nano C-waste, which act as fillers, thereby promoting cement hydration. This observation is consistent with XRD and FTIR analyses. However, when the concentration of MWCNT and nano C-waste reaches 0.3%, the intensity of the endothermic peak at 90-170°C decreases. This can be attributed to the agglomeration of MWCNT and nano C-waste nearby the cement particles, resulting in partial

hydration of the cement grains and hindering the reaction of the cement, leading to the production of a reduced amount of hydrated product.

Figures 5B and 5D also illustrate the weight loss of CEMIII pastes containing different ratio of MWCNT and nano C-waste cured in tap water up to 28 days. The CEMIII pastes containing MWCNT giving the weight loss 3.09, 3.45 and 3.15% for 0, 0.1and 0.3%, respectively at the temperature 200°C. It gives the weight loss 3.09, 3.63 and 3.46 % for 0, 0.1and 0.3%; respectively at the temperature 200°C for the CEMIII pastes containing nano C-waste.

This data serves to demonstrate the magnitude of the concentration of CEMIII pastes that encompass MWCNT and nano C-waste, which integrates 0.1%. Conversely, the reduction in intensity can be observed when additional nano is introduced, as evidenced by the decline in the intensity of the endothermic peak for CEMIII pastes. The findings suggest that CEMIII pastes containing 0.1% nano C-waste exhibit heightened intensity within the range of 90-170 (with a weight loss of 3.63%), surpassing those containing 0.1% MWCNT (with a weight loss of 3.45%). This phenomenon can be attributed to the active functional groups residing on the surface of nano C-waste, which act as nucleation sites for the formation of cement hydration products. Consequently, these functional groups facilitate the attachment and production of C-S-H on the surface of the nano C-waste.

Figure 6 displays thermograms of CEMIII pastes incorporating 0 and 0.1% MWCNT and nano C-waste, which were subjected to temperatures of 300°C, 500°C, and 700°C. The outcomes demonstrate that the peaks of all cement mixes at temperature ranges of 70°C, 90-180°C, 450-500°C, and 680-750°C experience a decline after exposure to 1000°C. This decline can be assigned to the detrimental impact of high temperatures on the decomposition of hydration products, leading to a deterioration in strength.
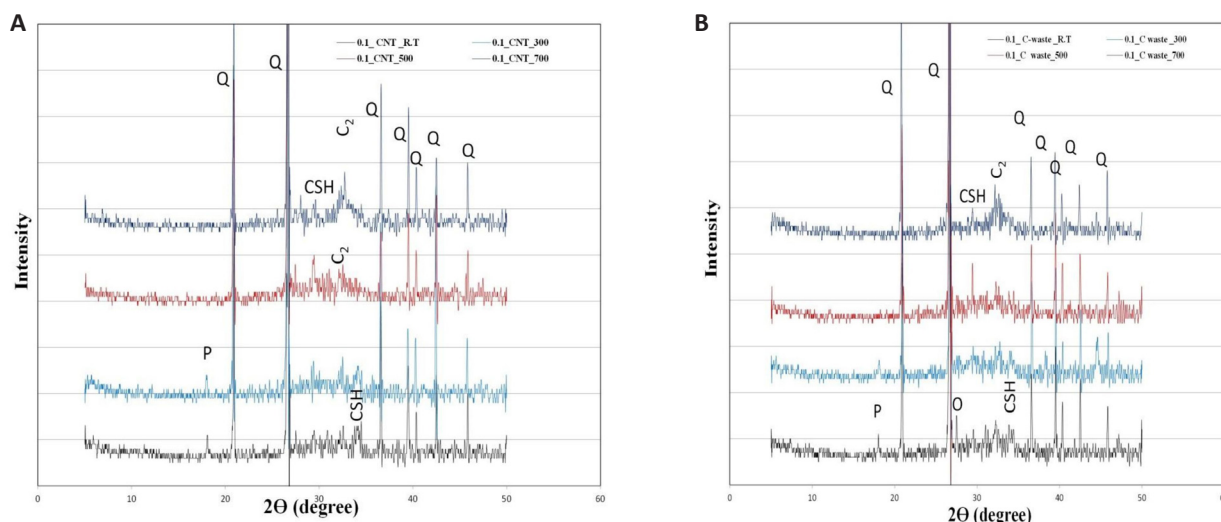
Figure 4. XRD pattern of fired CEMIII mortar mixes up to 700 degree and having. A: Various MWCNT doses. B: Various Nano-carbon wastes. [Q: Quartz, P:Portlandite, C2: dicalcium silicate, CSH: Calcium silicate hydrate, C3: tri calcium silicate, O: Orthoclase]
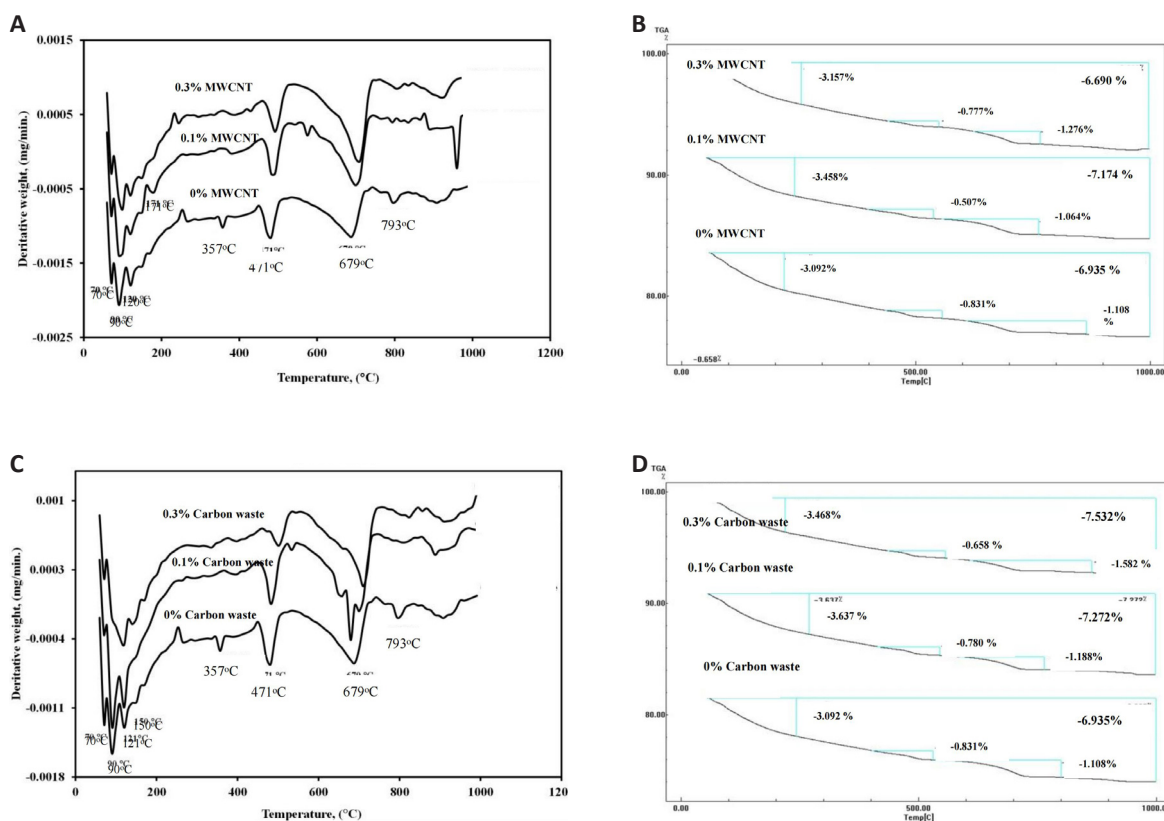
Figure 5. TGA& DTG pattern for MWCNT, Nano C-waste CEMIII mortar specimens. A&B: unfired MWCNT. C&D: unfired Nano C-waste.

Figure 6, specifically panels a and c, depict the augmentation in the intensity of the endothermic peak around 90-170℃ when 0.1% MWCNT and 0.1% nano C-waste are present, in comparison to the control mix. This augmentation occurs after exposure to elevated temperatures of 300℃, 500℃, and 700℃. The CEMIII paste containing 0.1% MWCNT exhibits weight losses of 0.99%, 0.46%, and 0.43%, while the CEMIII paste containing 0.1% nano C-waste demonstrates weight losses of 1.22%, 0.56%, and 0.32% at temperatures of 300℃,

500℃, and 700℃, respectively. In contrast, the control mix exhibits weight losses of 0.90%, 0.39%, and 0.34% at the same temperatures, as shown in Figure 6, panels B and D.

The findings indicate that the CEMIII paste containing 0.1% nano C-waste experiences the highest weight loss within the temperature range of 90-180℃, when exposed to elevated temperatures up to 700℃. This weight loss surpasses that of the CEMIII mixes containing 0 and 0.1% MWCNT. The cause for this can be ascribed to the physical
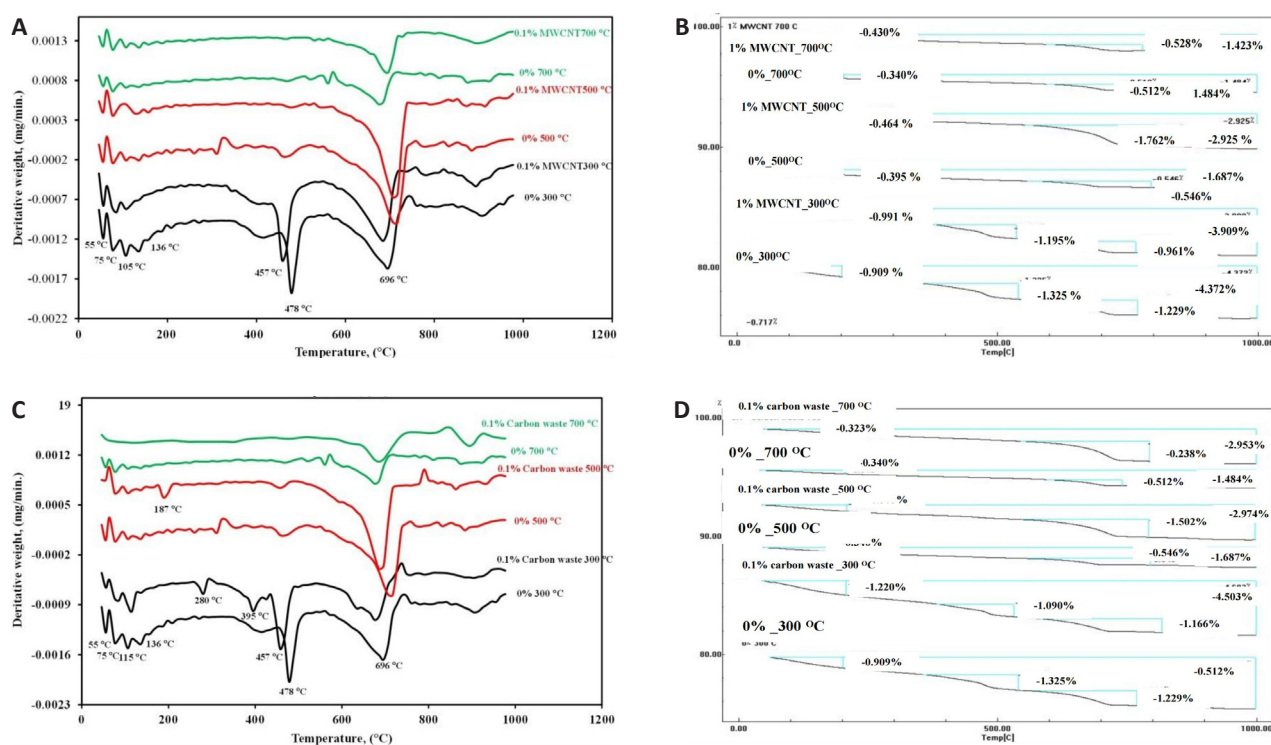
Figure 6. TGA& DTG pattern for MWCNT, Nano C-waste CEMIII mortar specimens. A&B: fired MWCNT. C&D: fired Nano C-waste.

and chemical impacts of the nano C-waste, which function as sites for the initiation of cement hydration substances, thus amplifying the adherence and formation of C-S-H.

3.3 Compressive Strength

Figure 7 exhibits the strength characteristics of C-waste and MWCNT cement-based composite that has been improved with varying ratios ranging from 0.1% to 0.7%. In our particular case, the enhancement of strength values for cement composites containing 0.1% MWCNT[37]. This dispersion is facilitated by the formation of strong coordinate bonds between the -COOH groups of the super-plasticizer and calcium ions within the matrix, leading to the formation of a dense CSH binder[34,38]. However, it should be noted that the effectiveness of the used super-plasticizer decreases for MWCNT ratios higher than 0.1%, as it results in the agglomeration of the nano materials, thereby reducing the dissemination of 3-D network as observed from FTIR, XRD and DTG.

The effectiveness of MWCNT can be attributed to the formation of nucleation sites, which in turn enriches the medium with various activation sites for the growth of the hydration phase[39]. However, an overdose of MWCNT exceeding 0.10% has a negative impact due to increased agglomeration, resulting in increased porosity and deformation of the matrix.

Furthermore, the strength results for 90 days tap water optimized MWCNT (0.1%) reach approximately 68MPa, while for the composite mix enhanced with C-waste materials at the same ratio, the strength reaches about 73MPa. It is worth noting that the incorporation of nano

C-waste materials leads to a higher affinity for increasing the mechanical properties of the hardened pastes compared to other references[40,41].

Figure 8 illustrates the bulk density of hardened cement pastes with varying proportions of MWCNT and nano C-waste, ranging from 0 to 0.7%, and cured for a period of 28 days. The findings also indicate that the density values of the cement samples exhibit a significant increase with the augmentation of MWCNT and nano C-waste content up to 0.1%, followed by a decrease with further increase up to 0.7%. However, it is important to note that the density of these specimens remains higher than that of the control mix. Specifically, the density of the specimens composed of 0.1% MWCNT and 0.1% nano C-waste increases by 3.4% and 3.8% respectively, at 28 days compared to the control mix. The enhancement in bulk density values of the cement pastes containing MWCNT and nano C-waste is attributed to the fine particle size of nano carbon, which fills the pores between paste particles. In addition, the active functional groups on the surface of nano C-waste act as nucleation sites for cement hydration products, thus facilitating the attachment and formation of C-S-H on the nano C-waste surface. Consequently, a homogeneous and denser microstructure is formed[42]. As a result, both the strength and density of the cement mixes increase with the augmentation of MWCNT and nano carbon content up to 0.1%.

In Figure 9, the residual compressive strength of the hardened cement samples containing different ratios of MWCNT and nano C-waste is presented after exposure to elevated temperatures up to 700°C for duration of two hours, in comparison to the original compressive strength
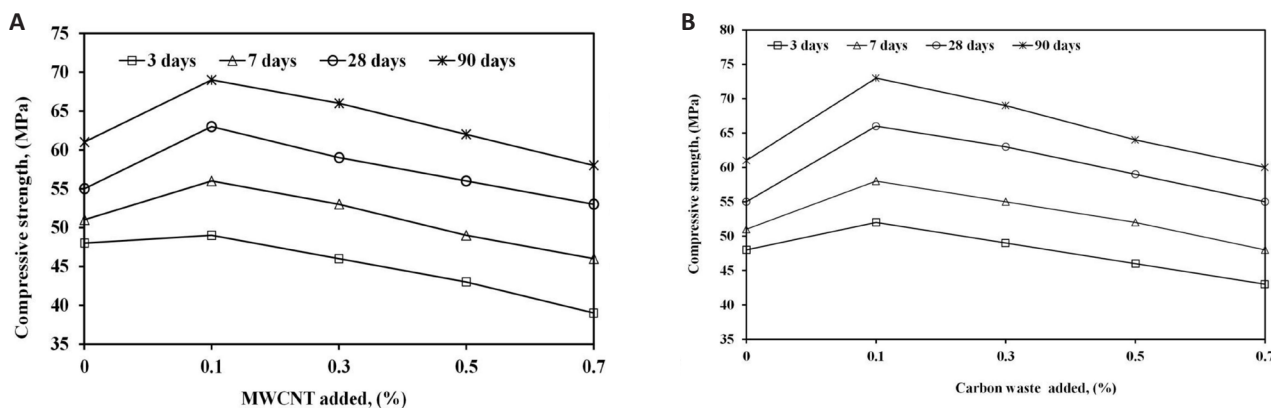
Figure 7. Compressive strength patterns of MWCNT and C-waste CEMIII mortar specimens cured up to 90 days.
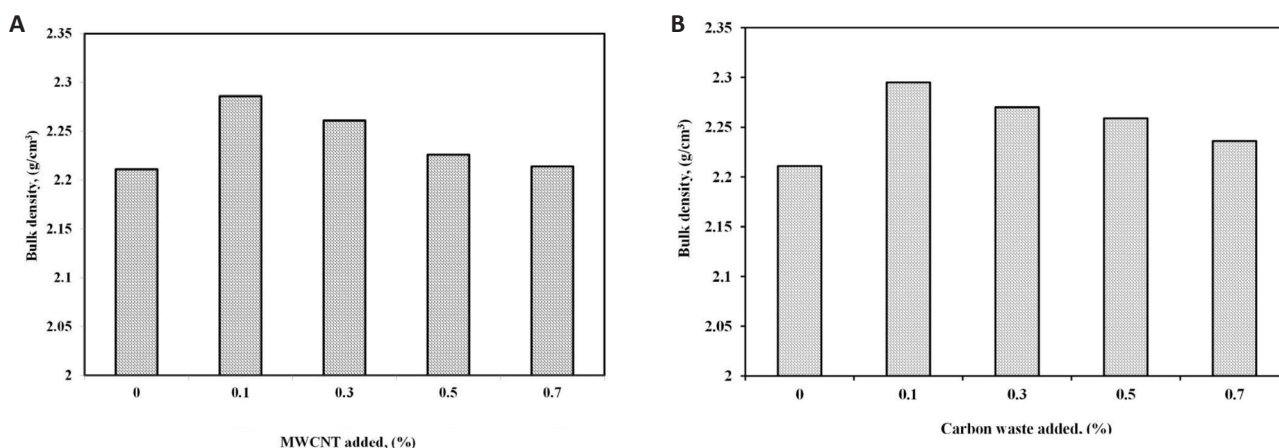
Figure 8. Bulk density patterns of 28 days MWCNT and C-waste CEMIII mortar specimens.

value prior to heating. The residual strength values of all cement samples with varying proportions of MWCNT and nano C-waste exhibit an increase after exposure to elevated temperatures up to 300°C. However, these values subsequently decrease with the increase in elevated temperatures up to 500°C and 700°C. Nevertheless, all mixes still display higher strength values compared to the cement mix without MWCNT and nano C-waste after exposure to elevated temperatures up to 500°C[43].

The strength values of all cement specimens, which encompass various proportions of MWCNT and nano C-waste, exhibited enhancement subsequent to exposure to heightened temperatures up to 300°C. This improvement can be predominantly attributed to the contraction of specimens and the augmentation in the intermolecular forces on the surface of gel particles as a result of the expulsion of absorbed moisture. Moreover, the active functional groups present on the surface of nano carbon serve as the sites for the initiation of cement hydration products, thereby expediting the rate of hydration. This acceleration further facilitates the adhesion and augmentation of hydration content in the cement specimens, leading to an increase in strength. Compressive strength decline with temperatures increase up to 700°C can be ascribed to the loss of crystalline water, along with alterations in morphology and the formation of micro-cracks under thermal fluctuations, subsequently resulting in thermal expansion of the specimens.

It can be noticed that the lower dose of MWCNT provide insufficient nucleation sites for CSH formation and accumulation which in turn can share in the adverse effect within the matrix. The previous explanation coincide with the increased MWCNT which leads to the agglomeration of the added nano-materials and hinder the propagation of CSH formation and accumulation. This explanation reflects the decreased strength of 0.5% than the control mix specially at higher firing temperatures as the degree of dehydration increased with temperature increase leading to formation of heterogeneous matrix.

Furthermore, the outcomes demonstrate that the strength values of cement specimens experience a rapid surge with an increase in the content of MWCNT and nano C-waste up to 0.1%, followed by a decline with a further increase in the content of MWCNT and nano C-waste up to 0.7%. However, even at elevated temperatures up to 700°C, the hardened cement specimens containing 0.5% MWCNT and 0.5% nano C-waste exhibit higher strength values compared to the cement mixture without MWCNT and nano C-waste. Additionally, the compressive strength of cement paste with 0.1% MWCNT experiences an increase of 3.6%, 6.3%, and 14% respectively, in comparison to the
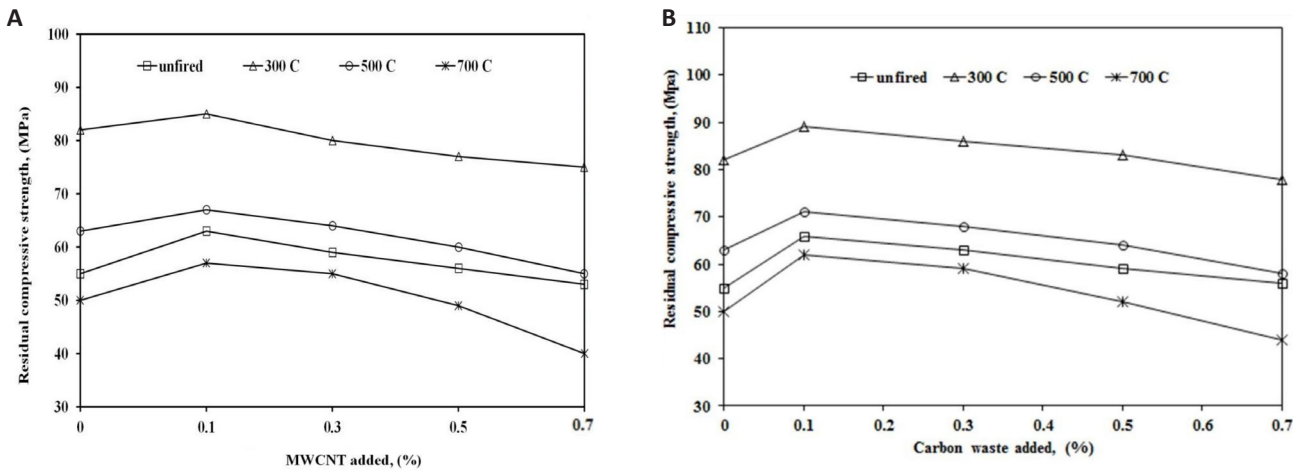
Figure 9. Residual strength patterns after firing up to 700 °C for MWCNT and C-waste CEMIII mortar specimens.
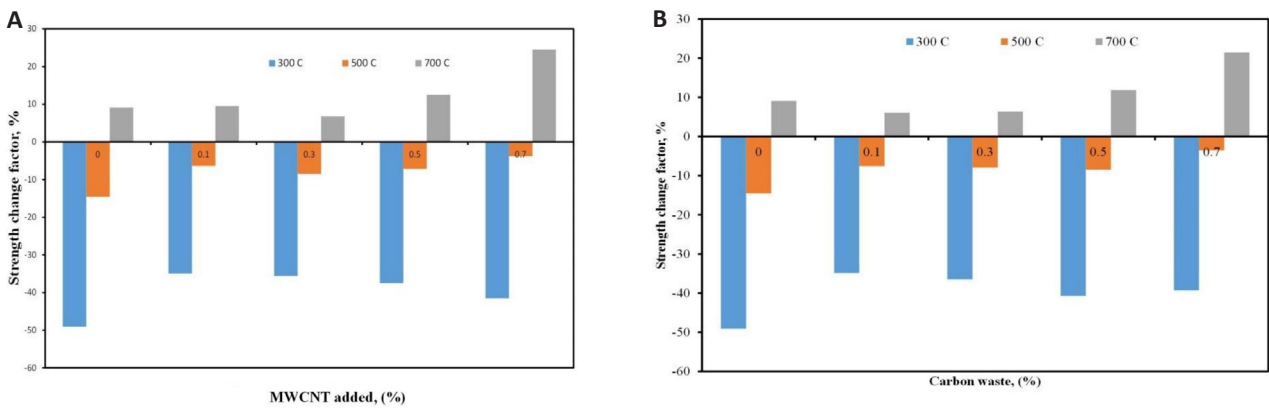
Figure 10. SCF patterns after firing up to 700 °C for MWCNT and C-waste CEMIII mortar specimens.

control mixture, after being exposed to temperatures of 300, 500, and 700°C. Similarly, the values of cement paste's strength with 0.1% nano C-waste exhibit an increase of 8.5%, 12.7%, and 24% respectively, in comparison to the control mixture, after exposure to temperatures of 300, 500, 700°C. It is evident that the cement paste containing 0.1% nano C-waste demonstrates higher compressive strength compared to the cement paste containing 0.1% MWCNT at all elevated temperatures up to 700°C.

The change in strength of fired cement composites that have been enhanced with nanomaterials, referred to as the SCF, is presented in Figure 10. This factor serves as a measure of the extent to which strength is either gained or lost when the cement composites are subjected to varying temperatures. In the event of Nano-glass being unavailable, the presence of adverse SCF values detected in the concrete specimens denotes a notable augmentation in the compressive potency. This can be attributed to the presence of reaction products and crystallization salts that fill the voids within the specimens. This phenomenon has been well-documented by several researchers[44,45].

Figure 10 illustrates an increase in SCF as the temperature rises up to 500°C, with the exception of specimens fired at 700°C and activated with Nano-

enhanced powder[33]. Furthermore, the figure demonstrates a subsequent decrease in SCF as the temperature continues to rise up to 500°C, followed by a loss in strength observed at 700°C. This reduction in strength can be attributed to the continuous dehydration of the hydrated cement materials at high temperatures. The compressive strength pattern, which will be thoroughly discussed in the XRD section, further supports this observation.

In Figure 11, the visual examination of the compressive strength of hardened cement samples containing varying ratios of MWCNT and nano C-waste, subjected to firing temperatures of 300°C, 500°C, and 700°C for a duration of two hours, is presented. The results indicate that thermal treatment of the cement specimens up to 300°C does not result in any visible deterioration. At 500°C, the surface of the reference sample exhibits the appearance of fine micro cracks, accompanied by changes in color. This phenomenon can be attributed to the loss of crystalline water and the dehydration of $Ca(OH)_2$, which is formed during the hydration of OPC, into CaO. As a consequence, the paste experiences shrinkage and cracking. Additionally, upon cooling, CaO rehydrates into $Ca(OH)_2$ in the presence of moisture in the air, leading to re-expansion and disintegration of the paste. The cement samples containing MWCNT and nano C-waste do not exhibit visible
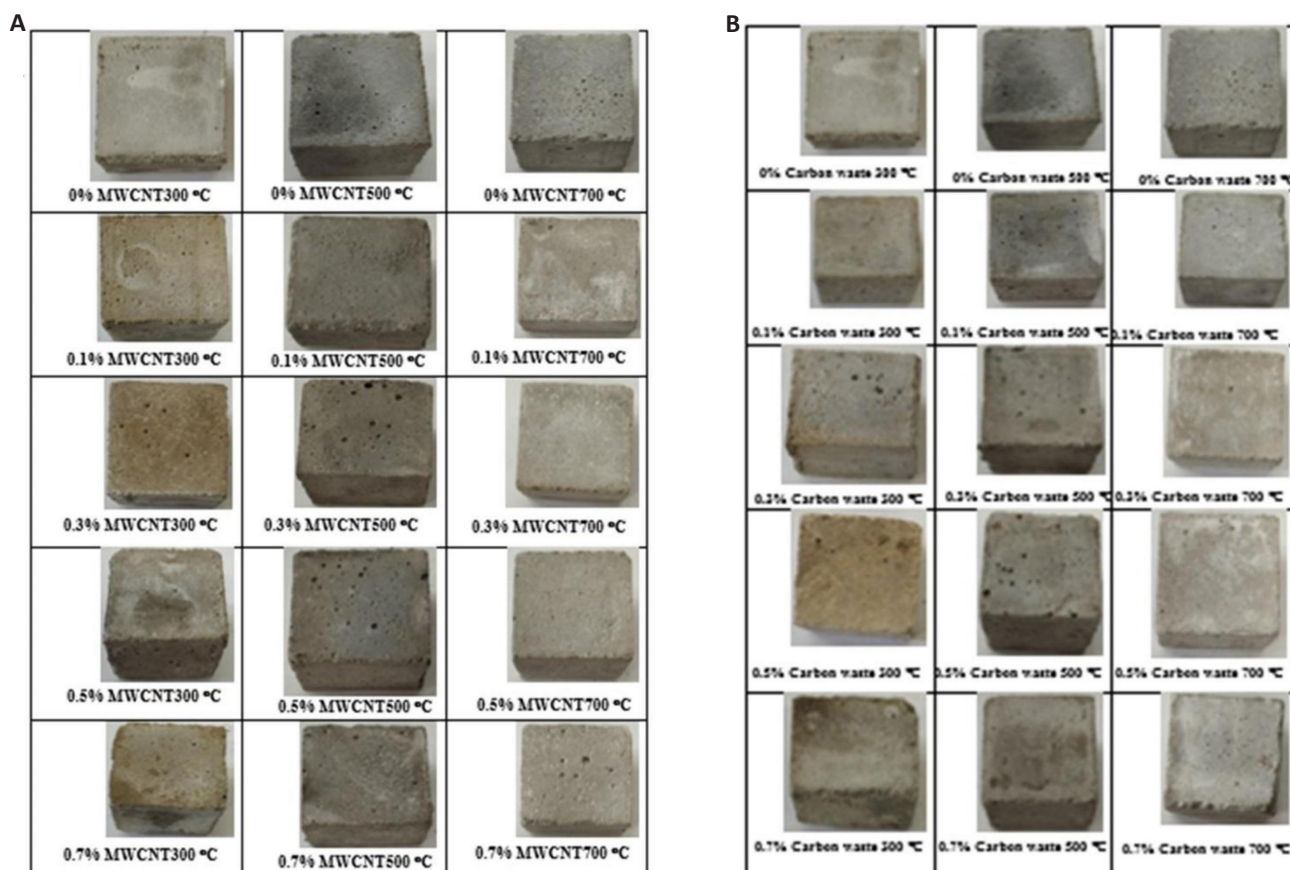
Figure 11. Visual examination. A: fired CEMIII mortar specimens incorporating MWCNT fired up to 700 degree. B: fired CEMIII mortar specimens incorporating C-waste fired up to 700 degree.

deterioration, except for some alterations in color. However, at higher temperatures, up to 700°C, extensive cracking and further deterioration become evident in all cement mixes. This can be attributed to the recrystallization of the amorphous phase present in the cement samples.

4 CONCLUSION

The results of this study possess a comparative study between the performance of multiwall carbon nanotube and C-wastes produced from aluminum production in the preparation of thermally stable cementitious mortar, where the main concluded remarks listed below:

(1) The incorporation of C-waste powder from aluminum production in preparation of cement composite possess high affinity in enhancing the physico- mechanical properties as compared with MWCNT nano-enhanced cement composites.

(2) Results confirmed the increased physicomechanical properties of C-waste than MWCNT in addition to its low production cost as compared with precious MWCNT.

(3) The produced cement mortar showed and enhanced thermal resistance up on firing up to 700 degree giving values of about 60MPa and 63MPa for MWCNT and C-waste.

(4) Results confirmed also, the increased thermal stability of C-waste than that of MWCNT in spite that both exceed the limits for thermal resistance mortar specification which is 60MPa.

(5) The increased thermal stability of C-waste than that of MWCNT in spite that both exceed the limits for thermal resistance mortar specification which is 60MPa[47].

(6) Moreover, XRD, FTIR, and DTG analyses have highlighted the increased activation of the formed cement, which forms additional CSH phases up to 15%, and decreases with further increments in the basalt ratio.

Acknowledgements
Not applicable.

Conflicts of Interest
The authors declared there is no conflict.

Author Contribution
Khater HM contribute for proposing the work of the paper, preparation of the materials, interpretation of the data, writing the manuscript as well as language editing. Gharieb M contribute for proposing the work of the paper, preparation of the materials, interpretation of the data, writing the manuscript as well as language editing.

Abbreviation List
C-waste, Carbon waste
C3S, Tricalcium silicate
CEMIII, Blended cement
CNTs, Carbon nano tubes
CSH, Calcium silicate hydrate

DTG, Differential thermal gravimetric analysis
MWCNT, Multiwall carbon nanotube
NMK,Nano metakaolin
OPC, Ordinary Portland cement
SCF, Strength change factor
TEM, Transmission electron microscopy

References

[1] Wu Z, Shi C, Khayat KH et al. Effects of different nanomaterials on hardening and performance of ultra-high strength concrete (UHSC). *Cement Concrete Comp*, 2016; 70: 24-34.[DOI]

[2] Iijima S. Helical microtubules of graphitic carbon. *Nature*, 1991; 354: 56-58.[DOI]

[3] Konsta-Gdoutos MS, Metaxa ZS, Shah SP. Multi-scale mechanical and fracture characteristics and early-age strain capacity of high performance carbon nanotube/cement nanocomposites. *Cement Concrete Comp*, 2010; 32: 110-115.[DOI]

[4] Liew KM, Kai MF, Zhang LW. Carbon nanotube reinforced cementitious composites: An overview. *Compo Part A-Appl S*, 2016; 91: 301-323.[DOI]

[5] Chaipanich A, Nochaiya T, Wongkeo W et al. Compressive strength and microstructure of carbon nanotubes-fly ash cement composites. *Mat Sci Eng A*, 2010; 527: 1063-1067.[DOI]

[6] Nochaiya T, Chaipanich A. Behavior of multi-walled carbon nanotubes on the porosity and microstructure of cement-based materials. *Appl Surf Sci*, 2011; 257: 1941-1945.[DOI]

[7] Morsy MS, Alsayed SH, Aqel M. Hybrid effect of carbon nanotube and nano-clay on physico-mechanical properties of cement mortar. *Constr Build Mater*, 2011; 25: 145-149.[DOI]

[8] Li G, Wang P, Zhao X. Mechanical behavior and microstructure of cement composites incorporating surface-treated multi-walled carbon nanotubes. *Carbon*, 2005; 43: 1239-1245.[DOI]

[9] Mudasir P, Naqash JA. Impact of carbon Nano tubes on fresh and hardned properties of conventional concrete. *Mater Today P*, 2023; 80: 1920-1925.[DOI]

[10] Siddique R, Mehta A. Effect of carbon nanotubes on properties of cement mortars. *Constr Build Mater*, 2014; 50: 116-129.[DOI]

[11] Konsta-Gdoutos MS, Metaxa ZS, Shah SP. Highly dispersed carbon nanotube reinforced cement based materials. *Cement Concrete Res*, 2010; 40: 1052-1059.[DOI]

[12] Chen SJ, Collins FG, MacLeod AJN et al. Carbon nanotube-cement composites: A retrospect. *IES J Part Civ Struct Eng*, 2011; 4: 254-265.[DOI]

[13] Carriço A, Bogas JA, Hawreen A et al. Durability of multi-walled carbon nanotube reinforced concrete. *Constr Build Mate*, 2018; 164: 121-133.[DOI]

[14] Yao Y, Lu H. Mechanical properties and failure mechanism of carbon nanotube concrete at high temperatures. *Constr Build Mater*, 2021; 297: 123782.[DOI]

[15] Khater HM, Nagar AEL. Evaluation of chloride resistance of silica fume and glass waste MWCNT-geopolymer composite. *Build Mater*, 2021; 2: 44-53.[DOI]

[16] Khater HM, Nagar AEL. Preparation of sustainable of eco-friendly MWCNT-geopolymer composites with superior sulfate resistance. *Adv Compos Hybrid Mat*, 2020; 3: 375-389.[DOI]

[17] Saafi M, Andrew K, Tang PL et al. Multifunctional properties of carbon nanotube/fly ash geopolymeric nanocomposites. *Constr Build Mater*, 2013; 49: 46-55.[DOI]

[18] Khater HM, Gawaad HAA. Characterization of alkali activated geopolymer mortar doped with MWCNT. *Constr Build Mater*, 2016; 102: 329-337.[DOI]

[19] Standard test method for compressive strength of hydraulic cement mortars. Annual book of ASTM standards. West Conshohocken, USA, 2019.

[20] Han B, Yu X, Ou J. Multifunctional and smart carbon nanotube reinforced cement-based materials. Springer: Berlin, Germany, 2011. Available at:[Web]

[21] Collins F, Lambert J, Duan W. The influences of admixtures on the dispersion, workability, and strength of carbon nanotube-OPC paste mixtures. *Cement Concrete Comp*, 2012; 34: 201-207.[DOI]

[22] Weitzel B, Hansen MR, Kowald TL et al. Influence of Multiwalled Carbon Nanotubes on the Microstructure of CSH-Phases: In Proceeding of 13th congress on the Chemistry of Cement. Madrid, Spain, 3-8 July 2011.[DOI]

[23] Hasanein SA, Khater HM, El-Enein SSA et al. Resistance of Alkali Activated Water-Cooled Slag Geopolymer to Sulphate Attack. *Ceram Siliconates*, 2011; 55: 153-160.[DOI]

[24] Saikia N, Usami A, Kato S et al. Hydration Behaviour of Ecocement in Presence of Metakaolin. Resour Proc, 2004; 51: 35-41.[DOI]

[25] Didamony E, Amer AA. Physico-chemical properties of supersulphated cement pastes. *Bull Fac Sci Zagazig Univ*, 2016; 38: 54-67.

[26] Guo W, Wu G, Wang J et al. Preparation and performance of geopolymers. *J Wuhan Univ Tech Mater Sci Ed*, 2008; 23: 326-330.[DOI]

[27] Khater HM, Abd El GHA. Effect of firing temperatures on alkali activated Geopolymer mortar doped with MWCNT. *Adv Nano Res*, 2015; 3: 225-242.[DOI]

[28] Concrete building units used in non-load and load bearing walls. Egyptian Organization for Standardization. Cairo, Egypt, 1992.

[29] Ugheoke BI, Onche E, Namessan ON et al. Property Optimization of Kaolin-Rice Husk Insulating Fire-Bricks. *Leonardo Electro J Pract Tech*, 2006; 9: 167-178.[DOI]

[30] Khater HM. Effect of nano-silica on microstructure formation of low-cost geopolymer binder. *Nanocomposites*, 2016; 2: 84-97.[DOI]

[31] Khater HM, Ezzat M. Preparation and characterization of engineered stones based geopolymer composites. *J Build Eng*, 2018; 20: 493-500.[DOI]

[32] Ganjian E, Pouya HS. Effect of magnesium and sulfate ions on durability of silica fume blended mixes exposed to the seawater tidal zone. *Cement Concrete Res*, 2005; 35: 1332-1343.[DOI]

[33] Bernal S, Gutierrez RD, Delvasto S et al. Performance of an alkali-activated slag concrete reinforced with steel fibers. *Constr Build Mater*, 2010; 24: 208-214.[DOI]

[34] Khater HM, Ghareeb M. Influence of nano-glass powder on the characteristics properties as well as stability against firing

for geopolymer composites. *Arab J Sci Eng*, 2023; 48: 8769-8783.[DOI]

[35] Jiang X, Kowald TL, Staedler T et al. Carbon nanotubes as a new reinforcement material for modern cement-based binders: Proceedings of the 2nd International Symposium on Nanotechnology in Construction. 2006.

[36] Chen J, Poon CS. Photocatalytic construction and building materials: from fundamentals to applications. *Build Enviro*, 2009; 44: 1899-1906.[DOI]

[37] Eldidamony H, Assal HH, Kandeel A et al. Utilization of Waste Hydrated Cement in Building Baterial: Proceedings of the 9th International Conference on chemistry and Its Role In Development (8th ICCRD). Mansoura & Sharm El-Sheikh, Egypt, 11-14 April 2005.[DOI]

[38] Heister E, Lamprecht C, Neves V et al. Higher dispersion efficacy of functionalized carbon nanotubes in chemical and biological environments. *ACS Nano*, 2010; 4: 2615-2626.[DOI]

[39] Peyvandi A, Soroushian P, Abdol N et al. Surface-modified graphite nanomaterials for improved reinforcement efficiency in cementitious paste. *Carbon*, 2013; 63: 175-186.[DOI]

[40] Khater HM. Effect of calcium on geopolymerization of aluminosilicate wastes. *J Mater Civil Eng*, 2012; 24: 92-101.[DOI]

[41] Khater HM. Effect of silica fume on the characterization of the geopolymer materials. *Int J Adv Struct Eng*, 2013; 5: 1-10.[DOI]

[42] Duxson P, Mallicoat SW, Lukey GC et al. The effect of alkali and Si/Al ratio on the development of mechanical properties of metakaolin-based geopolymers. *Colloids Surface A*, 2007; 292: 8-20.[DOI]

[43] Brown PW, Bothe JV. The stability of ettringite. *Adv Cem Res*, 1993; 5: 47-63.[DOI]

[44] Chaipanich A, Nochaiya T, Wongkeo W et al. Compressive strength and microstructure of carbon nanotubes-fly ash cement composites. *Mat Sci Eng*, 2010; 527: 1063-1067.[DOI]

[45] Carriço A, Bogas JA, Hawreen A et al. Durability of multi-walled carbon nanotube reinforced concrete. *Constr Build Mater*, 2018; 164: 121-133.[DOI]

[46] Lemougna PN, MacKenzie KJD, Melo UFC. Synthesis and thermal properties of inorganic polymers (geopolymers) for structural and refractory applications from volcanic ash. *Ceram Int*, 2011; 37: 3011-3018.[DOI]

[47] Standard Specification for Mortar for Unit Masonry. Standard ASTM. C270-19ae1. West Conshohocken, USA, 2019.